

## Epitaxial (001) BiFeO<sub>3</sub> membranes with substantially reduced fatigue and leakage

H. W. Jang,<sup>1</sup> S. H. Baek,<sup>1</sup> D. Ortiz,<sup>1</sup> C. M. Folkman,<sup>1</sup> C. B. Eom,<sup>1,a)</sup> Y. H. Chu,<sup>2</sup> P. Shafer,<sup>2</sup> R. Ramesh,<sup>2</sup> V. Vaithyanathan,<sup>3</sup> and D. G. Schlom<sup>3</sup>

<sup>1</sup>Department of Materials Science and Engineering, University of Wisconsin-Madison, Madison, Wisconsin 53706, USA

<sup>2</sup>Department of Physics and Department of Materials Science and Engineering, University of California, Berkeley, California 94720, USA

<sup>3</sup>Department of Materials Science and Engineering, Pennsylvania State University, Pennsylvania 16802-5005, USA

(Received 20 December 2007; accepted 20 January 2008; published online 14 February 2008)

We report substantially reduced fatigue and electrical leakage in BiFeO<sub>3</sub> membranes fabricated by releasing epitaxial (001) BiFeO<sub>3</sub> films from the Si substrates on which they were grown. Fatigue-free switching behavior of up to 10<sup>10</sup> cycles was observed for BiFeO<sub>3</sub> membranes with Pt top electrodes, while as-grown films break down at ~10<sup>9</sup> cycles. This is attributed to the low coercive field of BiFeO<sub>3</sub> membranes and their being free from substrate clamping. In contrast, (111) BiFeO<sub>3</sub> films exhibit significant fatigue at the same electric field. Epitaxial (001) BiFeO<sub>3</sub> membranes with low coercive field are very promising for lead-free ferroelectric memory and magnetoelectric devices. © 2008 American Institute of Physics. [DOI: 10.1063/1.2842418]

The lead-free perovskite BiFeO<sub>3</sub> has received considerable attention for nonvolatile memory applications because of its large polarization of ~100 μC/cm<sup>2</sup> along the [111] direction.<sup>1-4</sup> Epitaxial growth of BiFeO<sub>3</sub> on silicon has been demonstrated using an intervening epitaxial SrTiO<sub>3</sub> buffer layer.<sup>5</sup> The critical challenges remaining to be overcome before BiFeO<sub>3</sub>-based films will be candidates for integrated microelectronic devices are lowering its coercive field ( $E_c$ ) and leakage current and demonstrating its reliability.<sup>6</sup> Additionally, the multiferroic nature of BiFeO<sub>3</sub> offers the very exciting possibility of manipulating magnetic state by an electric field at room temperature.<sup>6</sup> Recently, Zhao *et al.* showed evidence of coupling between the ferroelectric and magnetic order parameters in BiFeO<sub>3</sub>.<sup>7</sup> The magnetoelectric coupling in BiFeO<sub>3</sub> has also been suggested to enable the switching of a ferromagnetic material such as (La,Sr)MnO<sub>3</sub> or Co coupled to the multiferroic through exchange interactions.<sup>8</sup>

In this paper, we demonstrate that the ferroelectric properties of epitaxial (001) BiFeO<sub>3</sub> thin films can be significantly enhanced by releasing them from the underlying Si substrate and transferring them onto a new substrate. (001) BiFeO<sub>3</sub> membranes with Pt top electrodes exhibit significantly lower  $E_c$ , lower leakage current, and improved fatigue in comparison to as-grown films. After release, fatigue-free switching behavior to 10<sup>10</sup> cycles was achieved for BiFeO<sub>3</sub> membranes. The mechanism of fatigue-free behavior in a (001) BiFeO<sub>3</sub> membrane is discussed and compared with both clamped (001) and (111) BiFeO<sub>3</sub> films.

Epitaxial (001) BiFeO<sub>3</sub> films were grown by off-axis radio-frequency (rf) magnetron sputtering<sup>3</sup> on (001) Si substrates miscut by 4° toward [110]. Prior to the deposition of the BiFeO<sub>3</sub> films, an epitaxial 15-nm-thick SrTiO<sub>3</sub> buffer layer and 100-nm-thick SrRuO<sub>3</sub> bottom electrode were deposited on the 50-μm thick Si substrates by molecular-beam

epitaxy<sup>9</sup> and 90° off-axis rf magnetron sputtering,<sup>10,11</sup> respectively. The fabrication process of epitaxial (001) BiFeO<sub>3</sub> membranes is described with schematic diagrams in Fig. 1. After epitaxial growth of BiFeO<sub>3</sub> films on the SrRuO<sub>3</sub>/SrTiO<sub>3</sub>/Si templates, Pt top electrodes (50-nm-thick and 100 μm in diameter) were formed on the BiFeO<sub>3</sub> film by rf sputtering and photolithography. After measurement of the electrical properties of the capacitors with the Pt top electrodes, the underlying Si substrate was completely removed by dry etching. In the etch process, the bottom SrTiO<sub>3</sub> and SrRuO<sub>3</sub> layers were used as etch stop layers. In order to handle the BiFeO<sub>3</sub> membranes, 25-μm-thick Au platforms were formed on the thin-film membranes using electroplating. In this way, capacitors of BiFeO<sub>3</sub> membranes with the same original Pt top electrodes were obtained and tested.

The lattice parameters and symmetries of the BiFeO<sub>3</sub> films before and after lift-off were determined by reciprocal

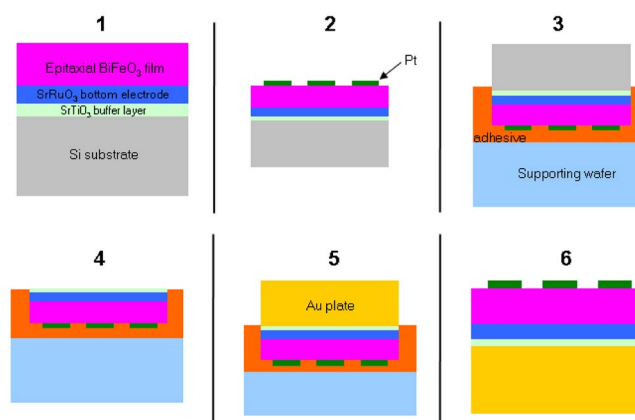


FIG. 1. (Color online) Schematic diagrams showing the fabrication process of strain-free BiFeO<sub>3</sub> membranes: (1) epitaxial growth of BiFeO<sub>3</sub>/SrRuO<sub>3</sub>/SrTiO<sub>3</sub>/Si heterostructures; (2) deposition of Pt top electrodes; (3) bonding the capacitor structure onto a supporting wafer; (4) removal of the Si substrate by inductive plasma etching; (5) Au electroplating; and (6) final structure after detachment of the membrane from the supporting wafer by dissolving the adhesive in acetone.

<sup>a)</sup> Author to whom correspondence should be addressed. Electronic mail: eom@engr.wisc.edu.

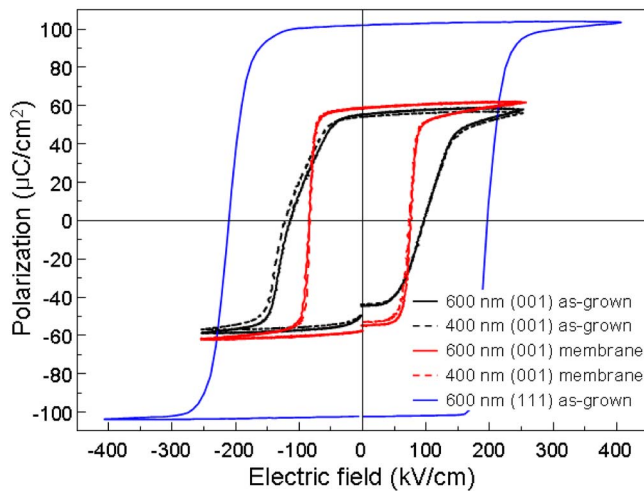


FIG. 2. (Color online)  $P$ - $E$  hysteresis loops of the 400-nm- and 600-nm-thick (001)  $\text{BiFeO}_3$  as-grown films and membranes. Both loops were obtained from the same Pt top electrode before and after lift-off. The  $P$ - $E$  hysteresis loop of a 600-nm-thick (111)  $\text{BiFeO}_3$  film on (111)  $\text{SrTiO}_3$  is shown for comparison.

space mapping using high-resolution x-ray diffraction; the details are reported elsewhere.<sup>12</sup> The as-grown films are subjected to biaxial tensile strains due to the large mismatch in the thermal expansion coefficients of Si and  $\text{BiFeO}_3$ .<sup>5</sup> For the membranes, the out-of-plane and in-plane lattice parameters are the same as those of bulk  $\text{BiFeO}_3$ , indicating that the  $\text{BiFeO}_3$  membranes are fully relaxed and strain-free. The strain relief accompanying lift-off results in a symmetry change of the  $\text{BiFeO}_3$  films from monoclinic for the as-grown strained films to rhombohedral for the membranes.

The ferroelectric properties were characterized by polarization-electric field ( $P$ - $E$ ) measurements. Figure 2 shows the  $P$ - $E$  hysteresis loops measured on 400-nm- and 600-nm-thick (001)  $\text{BiFeO}_3$  films on Si before and after lift-off. It should be noted that we measured the *same* Pt top electrode before and after lift-off, which excludes all other variables affecting  $P$ - $E$  hysteresis loops. It is apparent that the membranes display significantly enhanced ferroelectric properties, including increased remanent polarization ( $P_r$ ) and reduced  $E_c$ . The 400-nm-thick film on Si has a higher coercive field than the 600-nm-thick one. Both the 400-nm- and 600-nm-thick membranes, however, have almost the same coercive fields, which are 25%–30% lower than the clamped films. Achieving such low  $E_c$  values is a key to the use of  $\text{BiFeO}_3$  in nonvolatile memories. Notably, the  $E_c$  (80 kV/cm) of the membranes is the lowest ever reported for epitaxial  $\text{BiFeO}_3$  films<sup>1–3</sup> and comparable to those of epitaxial  $\text{Pb}(\text{Zr},\text{Ti})\text{O}_3$  films.<sup>11</sup> This observation implies that the relatively high  $E_c$  reported for epitaxial  $\text{BiFeO}_3$  thin films originates from a substrate-clamping effect. Meanwhile, (111)-oriented epitaxial  $\text{BiFeO}_3$  films on (111)  $\text{SrTiO}_3$  substrates show a large  $P_r$  (102  $\mu\text{C}/\text{cm}^2$ ) and very high  $E_c$  (200 kV/cm<sup>2</sup>).

To confirm the low  $E_c$  of the  $\text{BiFeO}_3$  membranes, we conducted piezoelectric force microscopy (PFM) measurements.<sup>13</sup> The results (not shown) revealed a two-domain stripe pattern with stripes separated by  $71^\circ$  domain walls in both the as-grown film and the  $\text{BiFeO}_3$  membrane, consistent with transmission electron microscopy analysis.<sup>3</sup> Furthermore, the lower  $E_c$  of the membrane is observed via

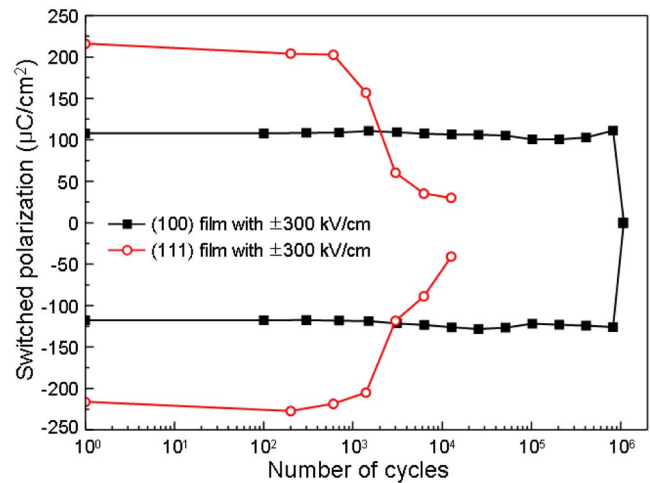


FIG. 3. (Color online) Fatigue characteristics of 600-nm-thick (001)  $\text{BiFeO}_3$ /(001) Si and (111)  $\text{BiFeO}_3$ /(111)  $\text{SrTiO}_3$  films. The width and frequency of switching pulses were 10  $\mu\text{s}$  and 100 Hz, respectively.

dc poling by the PFM tip. The polarization of the membrane was switchable by  $\pm 12$  V, whereas the bias had to be increased to  $\pm 20$  V to complete switching in the clamped film. This decrease in  $E_c$  for the membrane as determined by PFM poling is commensurate with the decrease observed in the  $P$ - $E$  loops. The discrepancy between both measurements is a result of switching on a local scale (PFM) versus the average switching observed under a patterned electrode ( $P$ - $E$  loop).<sup>3,13</sup>

Fatigue is one of the most important factors in determining the reliability of ferroelectric and magnetoelectric devices. We carried out fatigue tests on as-grown (001) and (111)  $\text{BiFeO}_3$  films by applying 5  $\mu\text{s}$  wide pulses with a repetition frequency of 100 Hz to the top Pt and bottom  $\text{SrRuO}_3$  electrodes, as shown in Fig. 3. The cycling voltage was selected to be  $\pm 300$  kV/cm, which gives complete switching for both films, as shown in Fig. 2. The capacitor of the (001)  $\text{BiFeO}_3$  film on Si shows no fatigue up to  $9 \times 10^5$  cycles and an abrupt break down at  $1 \times 10^6$  cycles. In contrast, the (111)  $\text{BiFeO}_3$  film on (111)  $\text{SrTiO}_3$  substrates exhibits a significant degradation in switching after  $10^4$  cycles, which is similar to the fatigue behavior typically seen in  $\text{Pb}(\text{Zr},\text{Ti})\text{O}_3$ .<sup>14</sup> The completely different fatigue behaviors between (001) and (111) films are consistent with the previous report on fatigue anisotropy. Bornand *et al.*<sup>15</sup> showed that (001)-oriented thin films of the rhombohedral relaxor ferroelectric  $\text{Pb}(\text{Yb}_{1/2}\text{Nb}_{1/2})\text{O}_3$ - $\text{PbTiO}_3$  have no fatigue ( $2P_r \sim 50 \mu\text{C}/\text{cm}^2$ ) up to  $10^{11}$  cycles, while (111) films exhibit a marked fatigue by voltage cycling.  $71^\circ$  domain switching occurs in the (001)  $\text{BiFeO}_3$  film, as shown in Fig. 3, while only  $180^\circ$  domain switching occurs in the (111)  $\text{BiFeO}_3$  film. This difference in domain switching leads to the fatigue anisotropy.<sup>15,16</sup>

We also conducted fatigue tests on the (001)  $\text{BiFeO}_3$  as-grown films and membranes at a switching field of  $\pm 160$  kV/cm. Figure 4(a) shows the fatigue characteristics of a 400-nm-thick (001) as-grown film and membrane. The amplitudes of the switched polarization for the as-grown films and membranes are very close to the  $2P_r$  values shown in Fig. 2, indicating that the switching field of  $\pm 160$  kV/cm provides complete switching in both cases. The capacitor of the as-grown film shows no fatigue up to  $9 \times 10^8$  cycles but

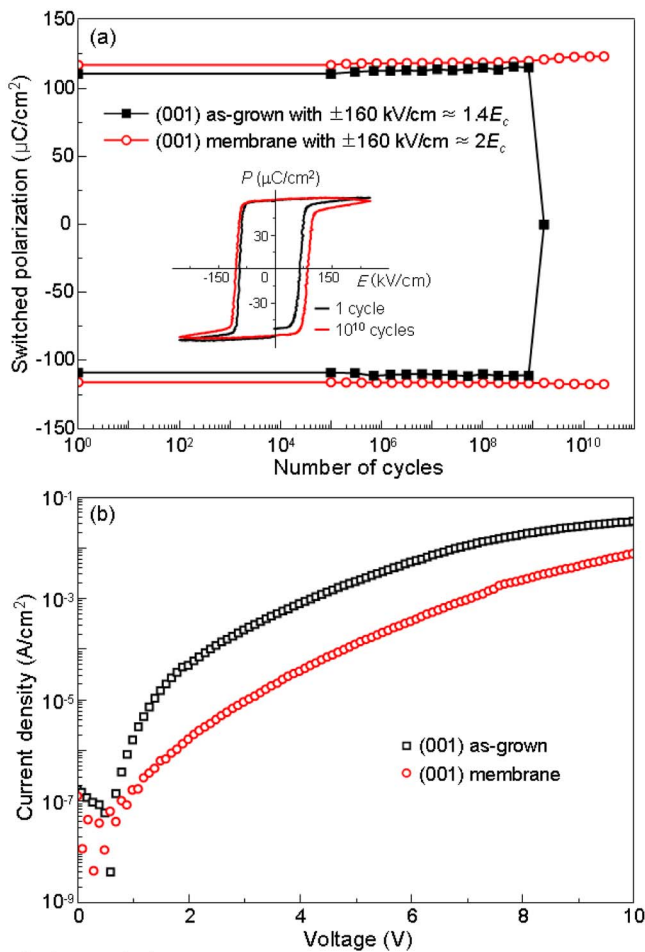


FIG. 4. (Color online) (a) Fatigue characteristics of a 400-nm-thick BiFeO<sub>3</sub> film and membrane. The width and frequency of the switching pulses were 5  $\mu$ s and 100 kHz, respectively. The inset shows  $P$ - $E$  hysteresis loops of the BiFeO<sub>3</sub> membrane before and after  $10^{10}$  cycles with a switching field of  $\pm 160$  kV/cm. (b) Forward leakage current characteristics as a function of applied voltage of 400-nm-thick BiFeO<sub>3</sub> thin film capacitors before (film) and after lift-off (membrane).

breakdown at  $1 \times 10^9$  cycles. In combination with the result in Fig. 4, we conclude that the lower switching field suppresses the breakdown of the film during the voltage cycling. In contrast, the BiFeO<sub>3</sub> membrane with Pt top electrodes remains fatigue-free to  $2.4 \times 10^{10}$  cycles. It is remarkable that  $2P_r$  of the BiFeO<sub>3</sub> membrane is as high as  $116 \mu\text{C}/\text{cm}^2$ , significantly higher than that of Pb(Zr<sub>0.53</sub>Ti<sub>0.47</sub>)O<sub>3</sub>,<sup>14</sup> SrBi<sub>2</sub>Ta<sub>2</sub>O<sub>9</sub>,<sup>17</sup> and Bi<sub>3.75</sub>La<sub>0.25</sub>Ti<sub>3</sub>O<sub>12</sub>.<sup>18</sup> For the 600-nm-thick membranes, we observed a very similar result, confirming the fatigue-free behavior of the BiFeO<sub>3</sub> membranes.

It is widely accepted that oxygen vacancies formed during growth, cause a portion of the Fe<sup>3+</sup> ions to become Fe<sup>2+</sup>, which is responsible for the high leakage current in BiFeO<sub>3</sub>.<sup>19</sup> From this, we suggest that the breakdown during the fatigue test could be due to the formation of conducting filaments as they gather mobile defects such as oxygen vacancies. After breakdown, observation under an optical microscope revealed a small dark spot on the Pt top electrode, which supports the formation of conducting filaments. Figure 4(b) shows that the membrane has a lower leakage current than the as-grown film. We believe that the reduction in the leakage current and easy domain wall motion that arises from freeing the BiFeO<sub>3</sub> film from substrate clamping prevents breakdown during the fatigue test and, thus, leads to

the observed fatigue-free behavior. Further study is needed to identify the mechanism responsible for the lower leakage current in the BiFeO<sub>3</sub> membranes.

In conclusion, we have demonstrated a significant enhancement of the ferroelectric properties of (001) BiFeO<sub>3</sub> thin films by removing the constraint of the underlying substrate. The reduction of both coercive field and leakage current and fatigue-free switching behavior over  $10^{10}$  cycles were achieved in strain-free BiFeO<sub>3</sub> membranes. This work presents a route to overcome some of the major challenges involved in applying BiFeO<sub>3</sub> thin films to nonvolatile memories and magnetoelectric devices. Another promising application of BiFeO<sub>3</sub> membranes is microelectronics built on flexible substrates. Using wafer bonding technology,<sup>20</sup> freestanding BiFeO<sub>3</sub> thin films can be integrated on any kind of flexible substrates, making it available for applications in displays, solar cells, smart cards, and rf tags.

The authors gratefully acknowledge the financial support of the National Science Foundation through grants ECCS-0708759 and DMR-0507146 and the Office of Naval Research through grants N00014-07-1-0215 and N00014-04-1-0426 monitored by Colin Wood.

- <sup>1</sup>J. Wang, J. B. Neaton, H. Zheng, V. Nagarajan, S. B. Ogale, B. Liu, D. Viehland, V. Vaithyanathan, D. G. Schlom, U. V. Waghmare, N. A. Spaldin, K. M. Rabe, M. Wuttig, and R. Ramesh, *Science* **299**, 1719 (2003).
- <sup>2</sup>J. F. Li, J. Wang, M. Wuttig, R. Ramesh, N. Wang, B. Ruetter, A. P. Pyatakov, A. K. Zvezdin, and D. Viehland, *Appl. Phys. Lett.* **84**, 5261 (2004).
- <sup>3</sup>R. R. Das, D. M. Kim, S. H. Baek, C. B. Eom, F. Zavaliche, S. Y. Yang, R. Ramesh, Y. B. Chen, X. Q. Pan, X. Ke, M. S. Rzchowski, and S. K. Streiffer, *Appl. Phys. Lett.* **88**, 242904 (2006).
- <sup>4</sup>D. Lebeugle, D. Colson, A. Forget, and M. Viret, *Appl. Phys. Lett.* **91**, 022907 (2007).
- <sup>5</sup>J. Wang, H. Zheng, Z. Ma, S. Prasertchoung, M. Wuttig, R. Droopad, J. Yu, K. Eisenbeiser, and R. Ramesh, *Appl. Phys. Lett.* **85**, 2574 (2004).
- <sup>6</sup>R. Ramesh and N. A. Spaldin, *Nat. Mater.* **6**, 21 (2007).
- <sup>7</sup>T. Zhao, A. Scholl, F. Zavaliche, K. Lee, M. Barry, A. Doran, M. P. Cruz, Y. H. Chu, C. Ederer, N. A. Spaldin, R. R. Das, D. M. Kim, S. H. Baek, C. B. Eom, and R. Ramesh, *Nat. Mater.* **5**, 823 (2006).
- <sup>8</sup>Y.-H. Chu, L. W. Martin, M. B. Holcomb, and R. Ramesh, *Mater. Today* **10**, 16 (2007).
- <sup>9</sup>L. V. Goncharova, D. G. Starodub, E. Garfunkel, T. Gustafsson, V. Vaithyanathan, J. Lettieri, and D. G. Schlom, *J. Appl. Phys.* **100**, 014912 (2006).
- <sup>10</sup>C. B. Eom, R. J. Cava, R. M. Fleming, J. M. Phillips, R. B. Vandover, J. H. Marshall, J. W. P. Hsu, J. J. Krajewski, and W. F. Peck, *Science* **258**, 1766 (1992).
- <sup>11</sup>C. B. Eom, R. B. Vandover, J. M. Phillips, D. J. Werder, J. H. Marshall, C. H. Chen, R. J. Cava, R. M. Fleming, and D. K. Fork, *Appl. Phys. Lett.* **63**, 2570 (1993).
- <sup>12</sup>H. W. Jang, S. H. Baek, D. Ortiz, C. M. Folkman, R. R. Das, Y. H. Chu, P. Shafer, J. X. Zhang, S. Choudhury, V. Vaithyanathan, Y. B. Chen, X. Q. Pan, D. G. Schlom, L. Q. Chen, R. Ramesh, and C. B. Eom (unpublished).
- <sup>13</sup>F. Zavaliche, P. Shafer, R. Ramesh, M. P. Cruz, R. R. Das, D. M. Kim, and C. B. Eom, *Appl. Phys. Lett.* **87**, 252902 (2005).
- <sup>14</sup>H. N. Alshareef, A. I. Kingon, X. Chen, K. R. Bellur, and O. Auciello, *J. Mater. Res.* **9**, 2968 (1994).
- <sup>15</sup>V. Bornand, S. Trolier-McKinstry, K. Takemura, and C. A. Randall, *J. Appl. Phys.* **87**, 3965 (2000).
- <sup>16</sup>J. F. Scott and M. Dawber, *Appl. Phys. Lett.* **76**, 3801 (2000).
- <sup>17</sup>C. P. de Araujo, J. Cuchiaro, L. McMillan, M. Scott, and J. Scott, *Nature (London)* **374**, 627 (1995).
- <sup>18</sup>B. H. Park, B. S. Kang, S. D. Bu, T. W. Noh, J. Lee, and W. Jo, *Nature (London)* **401**, 682 (1999).
- <sup>19</sup>X. Qi, J. Dho, R. Tomov, M. G. Blamire, and J. L. MacManus-Driscoll, *Appl. Phys. Lett.* **86**, 062903 (2005).
- <sup>20</sup>F. Niklaus, G. Stemme, J.-Q. Lu, and R. J. Gutmann, *J. Appl. Phys.* **99**, 031101 (2006).